Analytic tokamak equilibria with non-field aligned flows

Ap Kuiroukidis[1], G. N. Throumoulopoulos[2]

[1] *Technological Education Institute of Serres, 62124 Serres, Greece*

[2] *University of Ioannina, Association Euratom-Hellenic Republic, Physics Department, GR 451 10 Ioannina, Greece*

Introduction

It has been established in a number of fusion devices that sheared flows play a role in the transitions to improved confinement regimes as the L-H transition and the internal transport barriers (ITBs) (on ITBs formation in the JET and DIII-D devises see for example Refs. [1] and [2]). Equilibria with sheared flows which can be employed as starting points of stability and transport studies have been constructed on the basis of generalized Grad-Shafranov equations (GGSEs). In particular, linear analytical solutions to GGSEs are usually obtained by the method of separation of veriables.

A novel non-separable class of solutions describing up-down symmetric configurations with flows parallel to the magnetic field was found in Ref. [3] and was extended to include asymmetric configurations [4]. Since both velocity, components toroidal and poloidal, play a significant role in the transition to the improved confinement regimes, in the present contribution we will construct several classes of solutions for flows of arbitrary direction and examine their proprties in connection with the ITB phenomenology. Incompressible flows will be considered implying uniform density on magnetic surfaces, because the Alfvén Mach numbers (defined below) in large tokamks are low, i.e. on the order of 10^{-2}. The classes of analytic equilibria to be constructed include both separable and non separable solutions. They give nested magnetic surfaces, and their characteristics such as elongation and triangularity are in considerable accordance with actual geometrical and physical data that enter e.g. the ITER project. Some of the solutions are up-down asymmetric with a divertor X-point. Un-

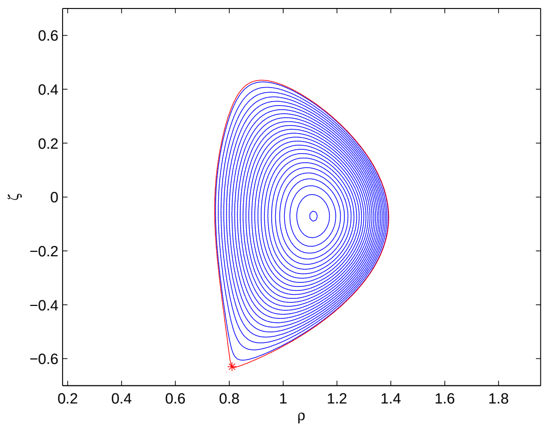

Figure 1: *ITER-like equilibrium of the linearized GGSE (3) for $P_2 = \Phi_2 = 0$ (Eqs. (4) and (5)). The bounding flux surface shown in red corresponds to $u_b = 2.18$ Wb, with $u_a = 0$ for the magnetic axis. The divertor X-point is located at $(\rho_X, \zeta_X) =$* $(0.81, -0.63)$.

fortunately, the linear stability of the solutions cannot be studied, unlike in Refs. [3] and [4] for parallel flows, due to the absence of a concise condition for equilibria with non-parallel flows. The results of the present study were published recently in Ref. [5]. Here we will present an extended summary.

Equilibria with non parallel flow

The stationary MHD equilibrium of a magnetically confined plasma with non parallel incompressible flow is governed by the GGSE [6, 7]

$$\Delta^* u + \frac{1}{2}\frac{d}{du}\left(\frac{X^2}{1-M_p^2}\right) + \mu_0 R^2 \frac{dP_s(u)}{du} + \frac{R^4}{2}\frac{d}{du}\left[\tilde{\rho}(\Phi'(u))^2\right] = 0 \quad (1)$$

together with the Bernoulli equation for the pressure

$$P = P_s(u) - \tilde{\rho}\left[\frac{v^2}{2} - R^2\left(\frac{d\Phi}{du}\right)^2\right]. \quad (2)$$

Here, the function $u(R,z)$ labels the magnetic surfaces (with z, R, ϕ cylindrical coordinates), $P_s(u)$ is the static (no flow) pressure, $X(u)$ is related to the toroidal magnetic field, $\Phi(u)$ is the electrostatic potential related to the non parallel component of flow, $\tilde{\rho}$ is the density, $M_p(u)$ is the Mach function of the poloidal velocity with respect to the poloidal Alfvén velocity and v is the velocity modulus. Owing to the flow, P in general is not a surface quantity. Once the free-function terms $X^2/(1-M_p^2)$, P_s and $d(\tilde{\rho}(\Phi'(u))^2)/du$ are specified, Eq. (1) can be solved under appropriate boundary conditions. We have chosen the free functions as $X^2(u)/(1-M_p^2) = X_0^2 + 2X_1 u + X_2 u^2$, $\mu_0 P_s(u) = P_0 - P_1 u - P_2 u^2/2$, $d\left[\tilde{\rho}(\Phi'(u))^2\right]/du = 2\Phi_1 + 2\Phi_2 u$ (where P_0, P_1, P_2, X_0, X_1, X_2, Φ_1, Φ_2 are free parameters the values of which will be assigned for specific equilibria) and introduce the dimensionless variables $\rho := (R/R_0)$, $\zeta := (z/R_0)$ where R_0 is the position of the geometric center. Then Eq. (1) assumes the form

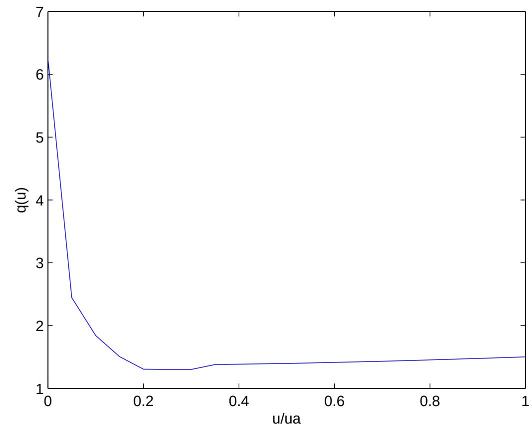

Figure 2: *Safety factor for a separable solution of (3) with $P_2 = \Phi_2 = 0$ and $X_0 = 90$, corresponding to a toroidal magnetic field of the order of $B_\phi \sim (X_0/R_a) = 15$ T. Note that the form of the safety factor is due to the fact that the outer bounding surface corresponds to $u = u_b = 0$.*

$$\frac{1}{R_0^2}[u_{\rho\rho} - \frac{1}{\rho}u_\rho + u_{\zeta\zeta}] + (X_1 + X_2 u) - R_0^2\rho^2(P_1 + P_2 u) + R_0^4\rho^4(\Phi_1 + \Phi_2 u) = 0. \quad (3)$$

We have constructed four classes of solutions to (3). It is emphasized that all the solutions hold for arbitrary densities and Mach functions. To construct completely particular equilibria we have made several choices of $\tilde{\rho}(u)$ and $M^2(u)$, e.g. $\tilde{\rho} = \tilde{\rho}_a \left(1-(u/u_b)^2\right)^{\lambda}$, $M_p^2 = M_a^2\left[1-(u/u_b)^n\right]$ or $M_p^2 = C(u-u_b)^n(u_a-u)^m$ with $C = M_a^2\left[\frac{m(u_a-u_b)}{m+n}\right]^{-m}\left[\frac{n(u_a-u_b)}{m+n}\right]^{-n}$. Here, the former M_p^2 is peaked on- while the latter is peaked off-axis in connection with respective auxiliary heating of tokamaks; u_b refers to the plasma boundary, the free parameters $\tilde{\rho}_a$ and M_a^2 correspond to the maximum values of $\tilde{\rho}$ and M_p^2 and m and n are related to the flow shear. One class of the solutions corresponding to $P_2 = \Phi_2 = 0$ is written as $u = u_1 + u_2$, where ($g := X_2R_0^2$)

$$\begin{aligned} u_1 &= \frac{P_1R_0^2}{X_2}\rho^2 - \frac{X_1}{X_2} + c_1 sin[\sqrt{g}(\rho^2+\zeta^2)^{1/2}] + +c_2 cos[\sqrt{g}(\rho^2+\zeta^2)^{1/2}] + c_3 cos[\sqrt{g}\zeta] \\ &\quad + c_4\rho^2 cos[\sqrt{g}\zeta] + c_5 sin[\sqrt{g}\zeta] + c_6\rho^2 sin[\sqrt{g}\zeta] + c_7\rho J_1(\sqrt{g}\rho) + c_8\rho Y_1(\sqrt{g}\rho), \quad (4) \end{aligned}$$

is the parallel-flow contribution (i.e. solution of Eq. (3) with $\Phi_1 = \Phi_2 = P_2 = 0$), and

$$u_2 = \frac{\pi R_0^6\Phi_1}{4g}\Big[-8\rho^4 J_3(\sqrt{g}\rho)Y_1(\sqrt{g}\rho) + \sqrt{g}\rho^5 J_4(\sqrt{g}\rho)Y_1(\sqrt{g}\rho) + g\rho^6 J_1(\sqrt{g}\rho)G1\Big] \quad (5)$$

is a solution of $u_{\rho\rho} - (1/\rho)u_\rho + gu + \Phi_1R_0^6\rho^4 = 0$. Here, $J_n(x)$, $Y_n(x)$ are the Bessel functions of the first and second kind respectively and of order n;

$$G1 = G\left(\{\{\frac{-3}{2}\},\{-1\}\},\{\{\frac{-1}{2},\frac{1}{2}\},\{\frac{-5}{2},-1\}\};\frac{\sqrt{g}\rho}{2},\frac{1}{2}\right)$$

is the Meijer G-function [8]. An ITER-like configuartion in connection with this solution is given in Fig. 1. The elongation of this configuration is $\kappa = 1.64$ and its triangularity is $\delta = 0.513$. The other three classes of solutions are given in Ref. [5].

On the basis of the solutions constructed we have examined certain equilibrium characteristics by means of the safety factor, electric field, toroidal velocity, Shafranov shift, current density and pressure. The most significant result is the following: The safety factor profile can be either monotonically increasing from the magnetic axis to the plasma boundary or can have a minimum associated with a slight reversal of the magnetic shear (Fig. 2). In all cases for a given value of the safety factor on magnetic axis ($q_a \geq 1$ so that the Kruscal-Shafranov limit is satisfied), the edge safety factor decreases as the magnitude of the electric field increases in connection with the parameters Φ_1 and Φ_2 as it is shown in Fig. 3. On the other side, the electric field results in an increase of the toroidal velocity $\mathbf{v}_\phi$ and its shear as can be seen in Fig. 4.

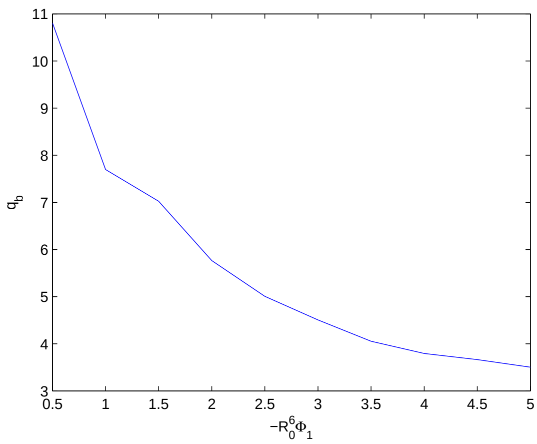

Figure 3: *Dependence of the edge (boundary) safety factor q_b on the parameter Φ_1, for $q_a = 1$, for the non separable solution of (3) (Eqs. (4) and (5)).*

These characteristics indicating a stabilizing effect of the electric field are qualitatively consistent with a past equilibrium study in cylindrical geometry [9] according to which the reversed magnetic shear and sheared poloidal and toroidal flow may act synergetically in the formation of ITBs. A synergism of reversed magnetic shear and sheared poloidal and toroidal rotation, consisting in that on the one hand the reversed magnetic shear plays a role in triggering the ITBs development while on the other hand the sheared rotation has an impact on the subsequent growth and allows the formation of strong ITBs, was observed in JET [1] and and DII-D [2].

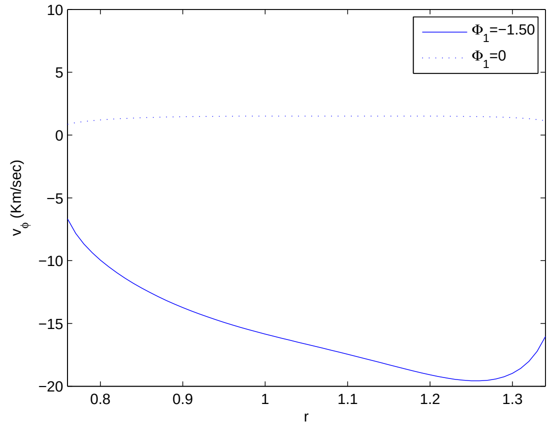

Figure 4: *Toroidal velocity for the equilibrium of Fig. 1, with* $\Phi_1 = -1.50$, $\Phi_1 = 0.0$, $\lambda = 0.5$ *and* $\rho_a = 1.0$.

References

[1] P. C. de Vries, E. Joffrin, M. Brix C. D. Challis, K. Crombé, B. Esposito et al., Nucl. Fusion **49**, 075007 (2009).

[2] M. W. Shafer, G. R. McKee, M. E. Austin K. H. Burrell, R. J. Fonck, and D. J. Schlossberg, Phys. Rev. Lett. **103**, 075004 (2009).

[3] Ap Kuiroukidis, Plasma Phys. Control. Fusion **52**, 015002 (2010).

[4] Ap Kuiroukidis and G. N. Throumoulopoulos, Phys. Control. Fusion **53**, 125005 (2011).

[5] Ap Kuiroukidis and G. N. Throumoulopoulos, Phys. Plasmas **19**, 022508 (2012).

[6] H. Tasso and G. N. Throumoulopoulos Phys. Plasmas **4**, 2378 (1998).

[7] Ch. Simintzis, G. N. Throumoulopoulos and G. Pantis, Phys. Plasmas **8**, 2641 (2001).

[8] *Higher Transcedental Functions*, Vol. 1, A. Erdelyi, Editor (Mc Graw Hill N.Y. 1953).

[9] G. Poulipoulis, G. N. Throumoulopoulos and H. Tasso, Plasma Phys. Control. Fusion **46**, 639 (2004).